pISSN 1229-3008 eISSN 2287-6251
Progress in Superconductivity and Cryogenics
Vol.18, No.2, (2016), pp.42~47 http://dx.doi.org/10.9714/psac.2016.18.2.042

Development of cryogenic free-piston reciprocating expander utilizing phase controller

Jeongmin Cha*, Jiho Park, Kyungjoong Kim, and Sangkwon Jeong

Korea Advanced Institute of Science and Technology 291, Daehak-ro, Yuseong-gu, Daejeon, 34141, Republic of Korea

(Received 9 May 2016; revised or reviewed 15 June 2016; accepted 16 June 2016)

Abstract

A free-piston reciprocating expander is a device which operates without any mechanical linkage to a stationary part. Since the motion of the floating piston is only controlled by the pressure difference at two ends of the piston, this kind of expander may indispensably require a sophisticated active control system equipped with multiple valves and reservoirs. In this paper, we have suggested a novel design that can further reduce complexity of the previously developed cryogenic free-piston expander configuration. It is a simple replacement of both multiple valves and reservoirs by a combination of an orifice valve and a reservoir. The functional characteristic of the integrated orifice-reservoir configuration is similar to that of a phase controller applied in a pulse tube refrigerator so that we designate the one as a phase controller. Depending on the orifice valve size in the phase controller, the different PV work which affects the expander performance is generated. The numerical model of this unique free-piston reciprocating expander utilizing a phase controller is established to understand and analyze quantitatively the performance variation of the expander under different valve timing and orifice valve size. The room temperature experiments are carried out to examine the performance of this newly developed cryogenic expander.

Keywords : Free-piston, reciprocating type, cryogenic expander, orifice valve size, phase controller

1. INTRODUCTION

There are two kinds of cryogenic expanders; centrifugal type and positive-displacement type. The former one generally implies turbine expanders which can be sub-categorized into radial turbine or axial flow one. Modern centrifugal turboexpanders are commonly applied in cryogenic refrigerators or gas liquefaction plants for the purpose of increasing the system efficiency and sometimes constructed as companders that produce work by high pressure gas to compress low-pressure stream [1-3]. The latter one is classified into various types such as screw, scroll and reciprocating expanders [4-6]. They principally operate by the increase of closed volume containing a constant amount of high pressure fluid mass. Although the positive-displacement type has inherent valve loss, it is more suitable for expansion process of low flow rates and high pressure ratios [7-8]. Another non-J-T (Joule-Thomson) expansion device is a cryogenic ejector that has no mechanical moving part, which are mainly applied in jet refrigerators for the requirement of a high reliability.

The free-piston (floating piston) expander, which was first studied by R.E. Jones and J.L. Smith Jr. [9] and developed by J.L. Smith Jr. and et al., is an expander which eliminates a mechanical linkage to a conventional reciprocating piston [10]. The free-piston in the expander can freely oscillate due to pressure difference with less mechanical friction, but its position has to be properly adjusted. An active control system using multiple valves and reservoirs at the warm-end of the expander was proposed to manipulate the precise piston movement and developed by AMTI Inc. [11].

A. Multi-valve expander (AMTI)

The free-piston reciprocating expander using multiple solenoid valves and reservoirs at the warm-end was developed for the application of small-scale Collins cycle of helium liquefaction system. Motion of the piston in the expander is to be controlled by the sophisticated active control with four on/off valves and reservoirs as shown in Fig. 1 (a). The pressure controlling algorithm is the core scheme in the expander operation because the piston movement is only controlled by the pressure difference at two-ends of the piston. Each opening and closing of the valves are actuated by the pressure and the position signal of the piston. This kind of complex feedback-controlled valve operation may be obviated by a passively controlled piston. This paper proposes a novel configuration of the free-piston type expander so that it is to replace both multiple valves and reservoirs at the warm-end with a phase controller as shown in Fig. 1 (b). It does not accompany any active valve control system. This kind of configuration is first suggested in this paper and will be examined with the conceptual design, the numerical simulation model and the preliminary experiments in the next sections.

B. Phase controller of expander

The function of the phase controller which is a combination of a single orifice valve and a reservoir is

* Corresponding author: chachadoncha@kaist.ac.kr

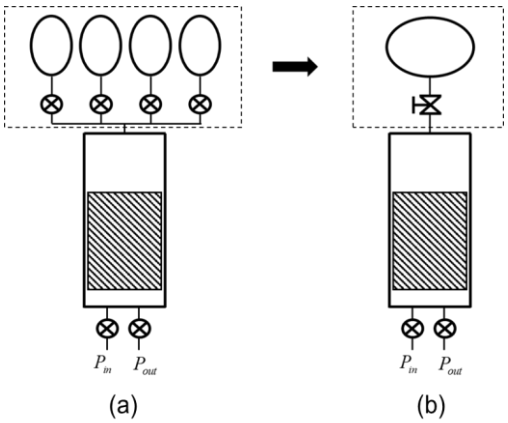

Fig. 1. Schematics of (a) multi-valve expander and (b) phase-controller expander**.**

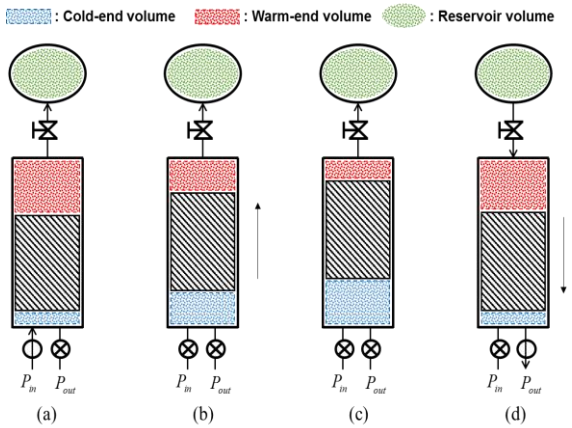

Fig. 2. Schematics of the expander cycle processes by each valve operation with piston movement**.**

similar to that applied in a pulse tube refrigerator. Depending on the orifice valve size in the phase controller, the pressure difference between the warm-end volume and the reservoir is generated. Its value varies due to the dynamically moving piston and the different resistance of the orifice size with a pressure phase difference between two volumes. We designate the following three cyclic processes of the new expander utilizing the phase controller as shown in Fig. 2.

(i) Intake process (a-b)

The expander cycle is initiated as the intake valve starts to open. Intake pressure is set to the higher pressure than that of the cold-end volume so that the pressurized gas flows into the cold-end volume pushing the free-piston up. Not only the pressure of the cold-end volume but also the pressure of the warm-end volume is increased due to the ascending piston caused by the pressure difference at the both ends of the piston. The pressure of the reservoir, however, does not immediately increase because of the orifice valve acting as a flow resistance. Thus, the pressure difference occurs between the warm-end and the reservoir volume, which is a potential for the cold-end volume to exert work by expansion.

(ii) Expansion process (b-c)

When the intake valve is closed (both valves are closed), the expansion process begins. Although the resistance of the orifice valve exists, the mass in the warm-end volume flows into the reservoir because of the prescribed pressure difference so that the cold-end volume expands continuously until the pressures of the warm-end and the reservoir come to equilibrium. After the equilibrium pressure, there is no fundamental driving force of expansion process but, slightly more gas-expansion can occur due to the inertia of the moving piston.

(iii) Exhaust process (c-d)

As the exhaust valve starts to open, the mass in the cold-end volume flows out of the expander due to the lower exhaust pressure. Both the cold-end and the warm-end pressures are decreasing rapidly, but the change of the reservoir pressure does not immediately occur due to the resistance, which is the same situation during the intake process. The exhaust valve is closed until the piston reaches the bottom of the cylinder, the exhaust process ends and a cycle is completed. The same processes are repeated and the cyclic steady state is obtained. With this intended operation, the PV work can be generated and most of the work done by the pressurized gas is mainly dissipated at the orifice valve at room temperature.

2. NUMERICAL SIMULATION

As mentioned above, the conceptual expander operation with the phase controller is feasible. We now have to consider the quantitative investigation and predict the expander performance in terms of thermodynamics and dynamics. In this model, several assumptions are made as follows.

(i) Working gas behaves as an ideal gas at equilibrium.
(ii) Both cylinder and piston are insulated (adiabatic).
(iii) Reservoir temperature is constant (isothermal).

The three aforementioned processes in the previous section progress quickly enough so that the adiabatic assumption is justified. The reservoir temperature can be assumed to be constant when the expander cycle reaches to a cyclic steady state, which implies that the dissipation of heat is equal to the amount of the generated PV work. For the analysis of this paper, each three individual control volume is separately considered; cold-end volume, warm-end volume and reservoir volume. All the thermodynamic states are determined by the energy conservation law (the first law of thermodynamics) as well as the mass balance.

A. Intake process

If we apply the energy conservation law to the cold-end volume neglecting kinetic and potential energy during the time step Δt, we can obtain (1) and it can be modified to (2) with the prescribed assumptions. Solving (2) for $P_{f,cold}$, we can obtain (3) which is a discretized form to find the final pressure after the time step Δt (i : initial, f : final).

$$\Delta E_{cold} = Q_{cold} - W_{cold} + (\Delta m \cdot h)_{in,cold} - (\Delta m \cdot h)_{out,cold} \quad (1)$$

$$\frac{c_v((PV)_f - (PV)_i)_{cold}}{R} = (-P_i(V_f - V_i) + (\Delta m c_p T)_{in} - (\Delta m c_p T)_{out})_{cold} \quad (2)$$

$$P_{f,cold} = \frac{1}{V_{f,cold}}(P_{i,cold}V_{i,cold} + (k-1)\cdot(-P_{i,cold}(V_{f,cold} - V_{i,cold}) + \Delta m_{in}c_p T_{in} - \Delta m_{out}c_p T_{cold})) \quad (3)$$

If we know both Δm_{in} which is the amount of mass-in through the intake valve and Δm_{out} which is the amount of mass-out by the clearance gap from the cold-volume to the warm-volume, the $P_{f,cold}$ can be calculated. Δm_{in} and Δm_{out} are determined by the mass flow equation of (4) and by the leakage equation of (5) [12-13]. Where, P_r is the pressure ratio of the cold-end volume divided by the intake pressure, k is the specific heat ratio, c is the radial clearance gap [m], μ_{visc} is the viscosity of the working fluid [Pa s], L_{piston} is the length of the piston [m], $D_{cylinder}$ is the diameter of the cylinder [m], R is the ideal gas constant [J kg^{-1} k^{-1}], P_{cold}, P_{warm} and T_{cold} are pressures [Pa] and temperature [K] at the specified control volume and $f_{correction}$ is the correction factor of each valve.

$$\frac{\Delta m_{in}}{\Delta t} = f_{correction}A_{in}P_{in}\left(\frac{2k}{k-1}P_r^{2/k}(1-P_r)^{(k-1)/k}\right)^{1/2} \quad (4)$$

$$\frac{\Delta m_{out}}{\Delta t} = \frac{\pi D_{cylinder}c^3(P_{cold}^{\ 2} - P_{warm}^{\ 2})}{12\mu_{visc}L_{piston}RT_{cold}} \quad (5)$$

Next, the displacement of the piston from the bottom of the cylinder is determined by using the dynamic equation of motion (6) during the time step Δt when the force generated by the pressure difference at two-ends of the piston is larger than the sum of the gravitational and friction force. Where, M_{piston} is the mass of the piston [kg], ΔP is the pressure difference at two-ends of the piston [Pa], A_{piston} is the cross sectional area of the piston [m^2], $F_{friction}$ is the friction force caused by the piston and cylinder [N], a is an acceleration of the piston [m s^{-2}], g is a gravitational acceleration [m s^{-2}], v is the velocity of the piston [m s^{-1}] and x is the displacement of the piston from the bottom of the cylinder [m].

$$a = \frac{1}{M_{piston}}(\Delta P A_{piston} - M_{piston}g - f_{friction})$$
$$\Delta v = a\Delta t \quad (6)$$
$$\Delta x = v\Delta t + \frac{1}{2}a\Delta t^2$$

When the physical states in the cold-end volume are determined at each time step from (1) to (6), the states of

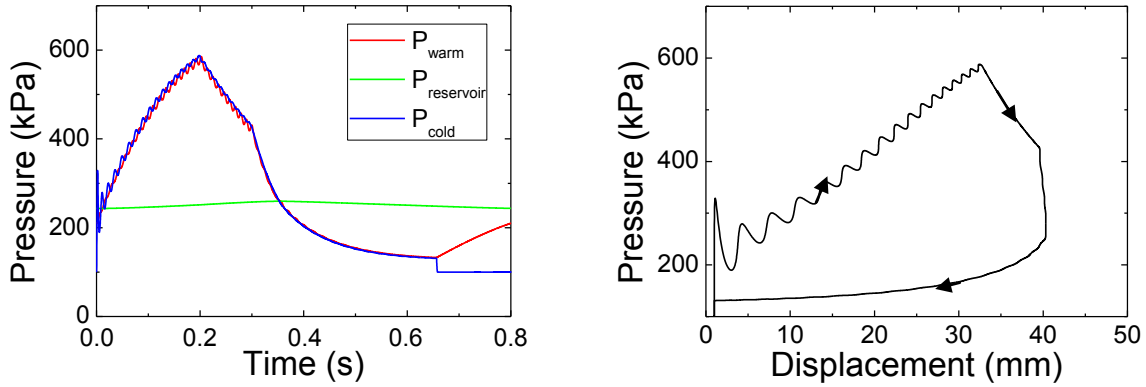

(a)

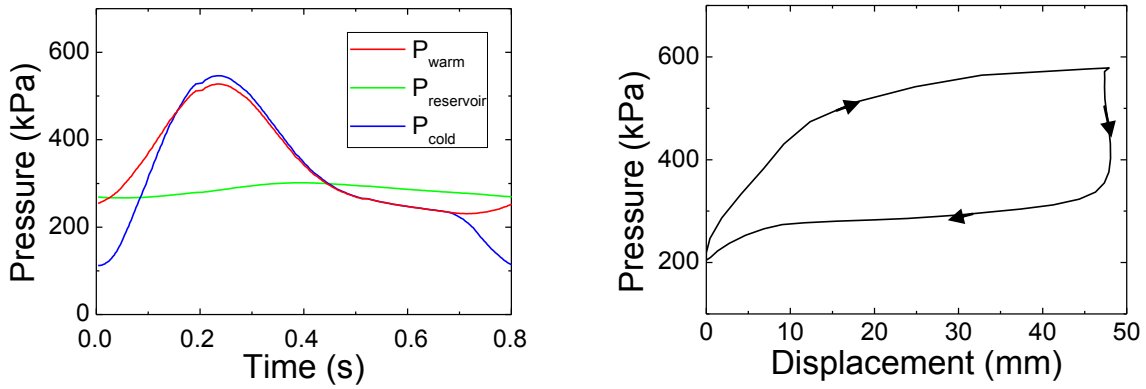

(b)

Fig. 3. (a) Simulation and (b) experimental results of the pressure-time and pressure-displacement curves in the case of t_{intake} = 0.2 s, $t_{expansion}$ = 0.1 s, $t_{exhaust}$ = 0.5 s, P_{intake} = 7 bar, $P_{exhaust}$ = 1 bar and 1.42 mm of the orifice valve size at cyclic steady state.

the next time step in the warm-end volume and the reservoir volume are consecutively determined step by step.

B. Expansion process

The difference between this expansion process and the intake process is that there is no mass flow into the cold-end volume through the intake valve. The mass change in the cold-end volume is only subject to the leakage by the clearance gap to the warm-end volume. Other procedures are same as those of the intake process.

C. Exhaust process

Exhaust process is the reverse of the intake process. Mass change in the cold-end volume is induced by the relatively higher pressure at the cold-end volume than that of the exhaust. Equation (7) is the same form with (3).

$$P_{f,cold} = \frac{1}{V_{f,cold}}(P_{i,cold}V_{i,cold} + (k-1)(-P_{i,cold}(V_{f,cold} - V_{i,cold}) - \Delta m_{in}c_pT_{cold} + \Delta m_{out}c_pT_{warm})) \quad (7)$$

When the three processes are finished, one cycle calculation is then completed and the next cycle with the same procedure begins. Number of cycles and each on/off valve opening periods are pre-set before the simulation runs. Table 1 shows the various parameters that can affect the expander performance which are separated into two

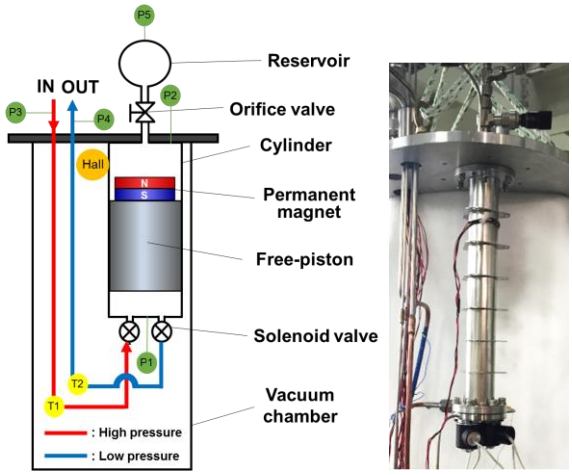

Fig. 4. Schematic diagram of experimental apparatus with the locations of sensors and a photo of experimental setup.

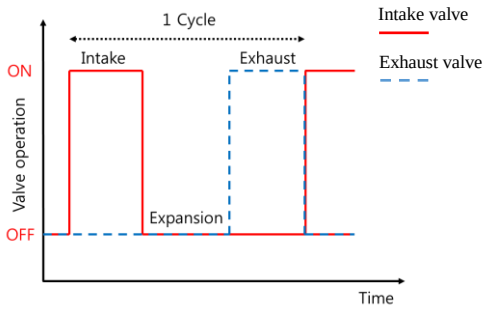

Fig. 5. Schematic diagram of on/off valve timing sequence at intake, expansion and exhaust period time.

TABLE 1
FIXED PARAMETERS AND OPERATING PARAMETER FOR THE EXPANDER SYSTEM.

Fixed parameters	Cylinder length and diameter	300 mm (L), 37.5 mm (D)
	Piston length and mass	250 mm (L), 0.3 kg
	Clearance gap	30 μm
	Reservoir temperature	300 K
	Working fluid	Argon gas
	Pressure ratio ($P_{intake}/P_{exhaust}$)	7
	Reservoir volume	0.5 L
	Intake period time	0.2 s
	Expansion period time	0.1 s
	Exhaust period time	0.5 s
Operating parameter	Orifice valve size	0 ~ 1.42 mm

categories: The fixed parameters and the operating parameters. In this paper, the values of the fixed parameters are selected by the experimental apparatus.

Fig. 3 (a) shows the simulation results of pressure variation and pressure-displacement in the case of 1.42 mm orifice valve size at cyclic steady state (specifically at the 1000th cycle). The numerical results show that the pressures at the cold-end, warm-end and the reservoir behave as expected in the conceptual design with the PV work generation of the cold-end. The simulation results are compared with the experimental results as shown in Fig. 3 (b). The major difference is the oscillation of the pressures at the warm-end and the cold-end, which cannot be found in the experimental results. It come from the less estimated leakage equation applied in the model, which consequently results in the higher inertia of the piston. Fig. 6 shows the attenuation of the pressure oscillation by increasing the radial clearance gap. When the leakage is small enough like in the case of c = 15 μm during the intake process, the cold-end pressure is rapidly increased due to the mass-in. However, the pressure of the warm-end is not following up because of the small leakage. In this case, pressure difference across the piston is increased so that both the acceleration of the piston and leakage are also increased. Thus, the cold-end pressure is rising by the time the acceleration effect is dominant and going down when the leakage effect is dominant. When the leakage is enough in the case of c = 45 μm, much less oscillation can be found. Thus, more realistic leakage equation that can reflect better is to be applied in the model later.

3. EXPERIMENT

A. Experimental apparatus

There are two main components in the experimental set. The first one is the expander system for low temperature achievement. A cylinder, free-piston, cold-end flange, two solenoid valves and several sensors are arranged inside a vacuum chamber as shown in Fig. 4. The cylinder and the piston are made of a thin-walled stainless steel tube and a phenolic tube respectively to minimize the conduction loss from the warm-end to the cold-end.

The clearance gap between the piston and the cylinder is approximately 30 μm to reduce leakage loss and friction simultaneously. At both sides of the cylinder, two flanges

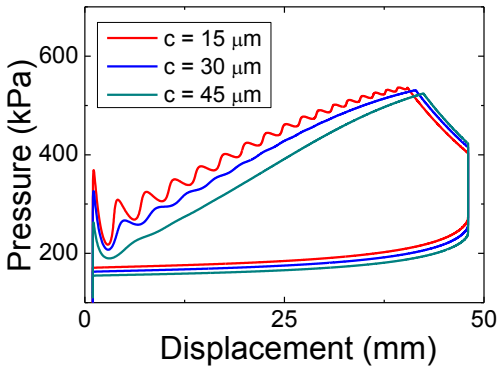

Fig. 6. Pressure-displacement curves by increasing the radial clearance gap as 15 μm, 30 μm and 45 μm.

(2.75 inch CF flange) are soldered. The cold-end flange is connected with another flange which is implemented with two on/off solenoid valves (B-Cryo Series, Gems Sensors & Controls) sealed by a copper gasket which is reliable at cryogenic temperature. The warm-end flange is connected to the top-flange sealed by a rubber O-ring.

The second part of the experimental apparatus is the phase controller which is a combination of an orifice valve and a reservoir located outside the vacuum chamber. The reservoir is made of a copper which has a high conductivity in order to dissipate the generated expansion work efficiently at ambient condition. The orifice valve

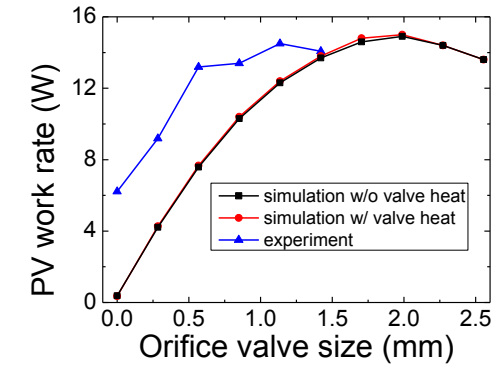

(a)

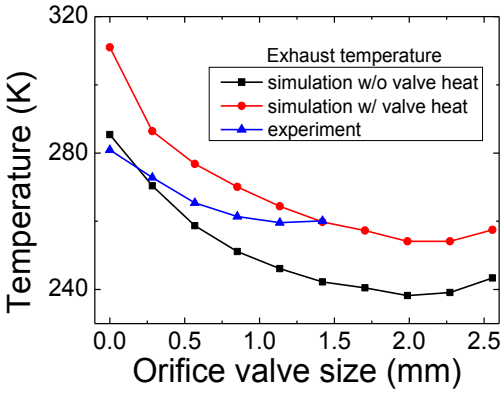

(b)

Fig. 7. (a) PV work rate curve and (b) the exhaust temperature curve at T_{intake} = 293.5 K depending on the orifice valve size.

(SS-4MG, Swagelok) is selected to accurately control the size of the orifice by number of turns open. Maximum orifice size is 1.42 mm and linearly changed by number of turns open.

Silicon diode temperature sensors (DT-670SD, Lake Shore Cryotronics) are installed to measure both inlet and exhaust temperatures. Pressures are measured at the inlet, outlet, cold-end, warm-end and reservoir. Piston position is also measured by use of Hall effect sensor. It is a transducer that varies its output voltage in response to a magnetic field [14]. In order to create magnetic field variation by the piston position change, a permanent magnet (Neodymium) is installed on the top of the piston and a Hall effect sensor is attached on the outside of the cylinder wall at the warm-end. The piston stroke (48 mm) from the bottom of the cylinder is thus instantaneously measured. All the sensors are indicated at each point as indicated in Fig. 4.

B. Experimental procedures and operating conditions

The expander experiment is conducted as an open-loop cycle. A pressurized gas at room temperature is delivered from a commercial gas cylinder and expands in the expander, then exhausts to atmosphere. There is an auxiliary volume between the gas cylinder and the expander inlet to maintain the inlet pressure constant. Before the expander operation, each on/off valve opening period at cold-end are set as shown in Fig. 5, the vacuum chamber is evacuated by vacuum pump and the orifice valve size is pre-set (from 1.42 mm to 0). Then, the expander operation starts and continues until its cycle comes to the cyclic steady state after number of cycles. All the data (pressure, piston position and temperature) are recorded by an NI data acquisition (DAQ) board (SCXI-1600 and SCXI-1125, National instrument) at a sampling rate of 50 Hz. The number of turns in the orifice valve is selected to find its optimal orifice valve size and therefore achieve the largest PV work or the lowest exhaust temperature.

C. Experimental results and discussions

The expander performance can be defined as follow;

$$\text{PV Work rate} = \frac{\text{PV work generation}}{\text{cycle time}}$$

Fig. 7 shows the experimental and simulation results by changing the orifice valve size at the same valve timing (t_{in} = 0.2 s, t_{exp} = 0.1 s, t_{exh} = 0.5 s). In the simulation model, however, it is more realistic to include a dominant parasitic heat because the on/off valves at the cold-end are actually in operation by the solenoids that generate joule-heating. Thus, we should estimate how much the valve heat has an effect on the exhaust temperature. In the cyclic steady state, the heat ingress to the cold-end cannot exceed the input power (I^2R = 8W) of the solenoid valve so that the value of 8 W of the valve heat is reflected in the simulation model and compared with the original one in Fig. 7. It indicates that the PV work rate and the exhaust temperature that are related to the expander efficiency are inversely proportional. Additionally, there exists an optimal point of

the orifice valve size at the specific valve timing. The optimal orifice valve size is 1.1 mm in the experiment and 2.0 mm in the simulation regardless of the valve heat consideration. Although the exact optimal points are different, the tendency that has the lowest T_{out} exists as to the orifice valve size. Since the orifice valve size over 1.42 mm is out of working range in the experiment, there are no data with the selected valve.

4. CONCLUSION

A new cryogenic free-piston reciprocating expander was proposed in this paper. The numerical model to predict the behavior of the expander utilizing the phase controller was developed and compared with the experiments. The expander performance in terms of the orifice valve size was mainly examined to see how the PV work rate and the exhaust temperature change. There exists an optimal point at specific valve timing so that adjustment of the orifice valve size is the key to the operation of this kind of the expander. From the experiments at room temperature (293.5 K) with argon gas, we found that the lowest exhaust temperature was observed as 259.6 K and calculated as 20% of the expander efficiency. The developed numerical model with experiments quantitatively suggests the possibility of utilizing the phase controller to cryogenic reciprocating expander.

ACKKNOWLEGMENT

This research is supported by a grant from Space Core Technology Development Program of National Research Foundation of Korea (NRF-2013-042033) funded by Ministry of Science, ICT & Future planning (MSIP).

REFERENCES

[1] Heinz Bloch and Claire Soares, *Turboexpanders and Process Applications*, Gulf Professional Publishing, pp. 42-84, 2001.

[2] Frank G Kerry, *Industrial Gas Handbook: Gas Separation and Purification*, CRC Press, 2007.

[3] Thomas Flynn, *Cryogenics Engineering*, vol. 2, CRC Press, pp. 652-664, 2005.

[4] G. Qiu, H. Liu and S. Riffat, "Expanders for micro-CHP systems with organic Rankine cycle," *Applied Thermal Engineering*, vol. 31, no. 16, pp. 3301-3307, 2011.

[5] B. Zhang, X. Peng, Z. He, Z. Xing and P. Shu, "Development of a double acting free piston expander for power recovery in transcritical CO 2 cycle," *Applied Thermal Engineering*, vol. 27, pp. 1629-1636, 2007.

[6] J. Manzagol, P. d'Harboullé, G. Claudet and G. G. Baguer, "Cryogenic scroll expander for claude cycle with cooling power of 10 to 100 Watts at 4.2 K," *ADVANCES IN CRYOGENIC ENGINEERING: Proceedings of the Cryogenic Engineering Conference-CEC*, AIP Publishing, pp. 267-274, 2002.

[7] V. Lemorta, L. Guillaumea , A. Legrosa , S. Declayea and S. Quoilina, "A comparison of piston screw and scroll expanders for small-scale rankine cycle systems," *The 3rd International Conference on Microgeneration and Related Technologies*, Belgium, 2013.

[8] H. J. Huff, D. Lindsay and R. Radermacher, "Positive Displacement Compressor and Expander Simulation," *International Compressor Engineering Conference*, Reinhard Radermacher Center for Environmental Energy, Maryland, 2002.

[9] R. E. Jones and J. Smith Jr, *Design and testing of experimental free-piston cryogenic expander*, Springer, 2000.

[10] C. Hannon, B. Krass, J. Gerstmann, G. Chaudhry, J. Brisson and J. Smith Jr, "Development of a Small-Scale Collins-Type 10 K Cryocooler for Space Applications," *Cryocoolers*, vol. 13, pp. 41-50, 2005.

[11] C. Hannon, B. Krass, J. Gerstmann, G. Chaudhry, J. Brisson, J. Smith Jr and T. Davis, "Development of a 4K-10K Collins-type cryocooler for space," *Optics & Photonics 2005*, International Society for Optics and Photonics, pp. 59040X-59040X-59012, 2005.

[12] B. Adrian, *Advanced Engineering Thermodynamics*, New York: John Wiley & Sons, 1969.

[13] K. Liang, M. W. Dadd and P. B. Bailey, "Clearance seal compressors with linear motor drives part i: background and system analysis," Proc.IMechE *J Power Energy*, vol. 227, no. 3, pp. 242-251, 2013.

[14] "The Hall Effect sensor," https://en.wikipedia.org/wiki/Hall_effect_sensor